

# Cavity Solitons in Driven VCSELs above Threshold

(Invited Paper)

G. Tissoni<sup>a</sup>, I. Protsenkob<sup>b</sup>, R. Kheradmand<sup>a,c</sup>, F. Prati<sup>a</sup>, M. Brambilla<sup>d</sup>, and L. A. Lugiato<sup>a</sup>

<sup>a</sup>INFM, Dipartimento di Scienze, Università dell'Insubria, Via Valleggio 11, 22100 Como, Italy.

<sup>b</sup>Lebedev Physics Institute, Moscow, Russia Scientific Center of Applied Research, JINR, Dubna, Russia

<sup>c</sup>Center for Applied Physics and Astronomical Research, University of Tabriz, Tabriz, Iran;

<sup>d</sup>INFM, Dipartimento di Fisica Interateneo, Università e Politecnico di Bari, Via Orabona 4, 70126 Bari, Italy.

**Abstract**— CSs have been theoretically predicted and recently experimentally demonstrated in broad area, vertical cavity driven semiconductor lasers (VCSELs) slightly below the lasing threshold. Above threshold, the simple adiabatic elimination of the polarization variable is not correct, leading to oscillatory instabilities with a spuriously high critical wave-number. To achieve real insight on the complete dynamical problem, we study here the complete system of equations and find regimes where a Hopf instability, typical of lasers above threshold, affects the lower intensity branch of the homogeneous steady state, while the higher intensity branch is unstable due to a Turing instability. Numerical results obtained by direct integration of the dynamical equations show that writable/erasable CSs are possible in this regime, sitting on unstable background

**Keywords:** cavity solutions, pattern formation, semiconductor lasers

## I. INTRODUCTION

The investigations in the field of spatial pattern formation in nonlinear optical systems offer an approach to parallel optical information processing, by encoding information in the transverse structure of the field [1]-[3].

The problem of the correlation among different parts of an optical pattern can be solved by generating spatial structures which are localized in a portion of the transverse plane in such a way that they are individually addressable and independent of one another. Cavity solitons (CSs) are single-peaked localized structures. They have been theoretically predicted [4]-[12] and experimentally observed in several classes of nonlinear resonators. Experimental observations in macroscopic cavities have been obtained in photorefractive resonators [13] and lasers with saturable absorbers [14]; similar phenomena have been observed in other systems with feedback [15]-[17].

Experimental observation of cavity solitons (CSs) in semiconductor micro-resonators is an important issue not only for fundamental physics but also for developing application-oriented devices. CSs have been recently experimentally demonstrated in broad area, vertical cavity, driven semiconductor lasers (VCSELs) slightly below the lasing threshold [18]. The device is driven by a broad area, coherent and stationary holding beam, and is operated under parametric conditions such that the output is basically uniform over an extended region. By injecting a localized laser pulse one can write a CS where the pulse

passes and the CS persists after the pulse, thanks to the feedback exerted by the cavity. The CSs written in this way can be erased by injecting again pulses in the locations where they lie; in most cases, these pulses must be coherent and out of phase with respect to the holding beam. It has been observed that when the current injection level was approximately equal or even slightly above the lasing threshold, the presence of CSs was not essentially affected. Therefore, we decided to extend the theoretical prediction and numerical simulation of such devices above threshold [19].

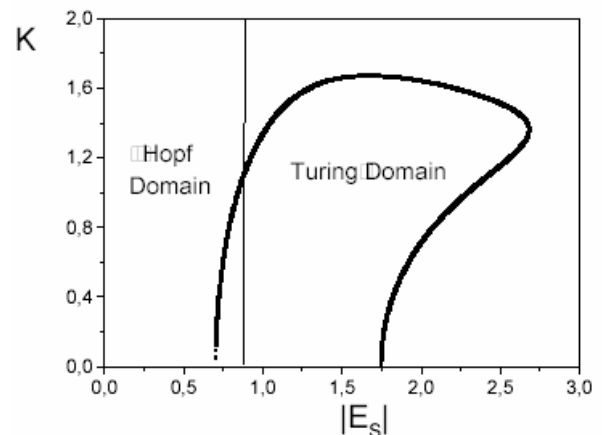


**Fig. 1** Turing and Hopf instability domains affecting the homogeneous steady state  $E_s$  for the case of simple adiabatic elimination (rate-equation approximation), for a driven semiconductor laser above threshold: the Hopf instability boundary is a vertical line, corresponding to an infinite number of unstable wave-vectors ( $K$  is the wave-vector of the perturbation). The model adopted here is that of Ref. [19].

In the case of a homogeneously broadened two level laser, it is well known that the simple adiabatic elimination of the polarization variable is not correct, leading to oscillatory instabilities with a spuriously high critical wave number [20]-[21]. The same happens in the case of a semiconductor laser with injected signal, when the current is increased above threshold. In Fig. 1 we show the instability domains obtained with the rate-equation model of Ref. 19 when we raise the injected current above the laser threshold. As a new feature, a Hopf domain appears above threshold, but it is delimited by a vertical line: this means that all the wave-vectors are unstable, that is clearly unphysical. More refined techniques, such as centre manifold adiabatic elimination, have been introduced in

the free-running laser case [22], but they can solve only partially the problem: specifically, they "work" only for negative values of the atomic detuning.

To achieve real insight on the complete dynamical problem, we decided to study the complete system of equations, by adopting a phenomenological model recently proposed by Tartwijk and Agrawal [22].

Section 2 is dedicated to the description of the Agrawal model, Section 3 is devoted to the homogeneous stationary solutions and the linear stability analysis. In Section 4 we report the numerical results on Cavity Solitons existence and on/off switching. Finally, conclusions are presented in Section 5.

## II. THE MODEL

We consider a broad area semiconductor VCSEL. The semiconductor micro-resonator is of the Fabry-Perot type, with a MQW structure perpendicular to the direction  $z$  of propagation of the radiation inside the cavity as in [19].

The model we adopt is a phenomenological model recently proposed by Tartwijk and Agrawal [22] for the free-running laser case. It describes a semiconductor laser with a macroscopic polarization, similar to a simple two level model (5 variables), but containing all the information concerning the physics of semiconductors. Dynamical equations can be cast in the following form:

$$\frac{\partial E}{\partial t} = -k[(1+i\theta)E - E_I - P - ia\nabla_{\perp}^2 E] \quad (1)$$

$$\frac{\partial P}{\partial t} = -\gamma_{\perp}[\Gamma(N) + i\Delta(N)][P - 2C(1-i\alpha)NE], \quad (2)$$

$$\frac{\partial N}{\partial t} = -\gamma_{\parallel} \left[ N - j + \frac{1}{2}(E^*P + EP^*) - d\nabla_{\perp}^2 N \right], \quad (3)$$

Where  $E$ ,  $P$  and  $N$  are the normalized electric field, macroscopic polarization and carrier density respectively,  $\kappa$  is the cavity damping constant,  $\gamma_{\perp}$  is the polarization decay rate, and  $\gamma_{\parallel}$  is the carrier non-radiative

recombination rate.  $\theta = \frac{\omega_c - \omega_0}{\kappa}$  is the cavity detuning parameter, with  $\omega_0$  being the frequency of the holding field and  $\omega_c$  the longitudinal cavity frequency closest to  $\omega_0$ . The transverse Laplacian, defined as usual as

$$\nabla_{\perp}^2 = \frac{\partial^2}{\partial x^2} + \frac{\partial^2}{\partial y^2},$$

represents diffraction in Eq. (1), and carrier diffusion in Eq. (3), through the diffraction and diffusion parameters  $a$  and  $d$ , respectively. The parameter  $E_I$  is the normalized injected field (taken real and positive for definiteness),  $j$  is the normalized injected current,  $C$  is the bistability parameter, and  $\alpha$  is the linewidth enhancement factor.

This model is characterized by the presence of an "effective" damping  $\Gamma(N)$  and detuning  $\Delta(N)$  in the macroscopic polarization equation. They depend on  $N$  and frequency, and by adopting a phenomenological approach, we assume  $\Gamma(N) + i\Delta(N) = 4.2(N+1) - i1.2$ , as in [24].

For a detailed derivation of the dynamical equations

(especially of Eq. (2)), see [23] and [24].

It is important to notice that if the polarization variable is adiabatically eliminated and its stationary value  $P_S$  is substituted in Eqs. (1) and (3), one gets exactly the model of Ref. [19].

## III. LINEAR STABILITY ANALYSIS OF THE HOMOGENEOUS STEADY STATE

We now approach the complete model described by the three space-time dependent PDEs (1), (2), and (3). The homogeneous solution  $(E_S, P_S, N_S)$  is obtained, as usual, by setting equal to zero all the temporal and spatial derivatives. We obtain:

$$|E_I|^2 = |E_S|^2 \left\{ \left[ 1 - \frac{2Cj}{1+2C|E_S|^2} \right]^2 + \left[ \theta + \frac{2Cj\alpha}{1+2C|E_S|^2} \right]^2 \right\}, \quad (4)$$

$$P_S = \frac{2Cj(1-i\alpha)E}{1+2C|E_S|^2}, \quad (5)$$

$$N_S = \frac{j}{1+2C|E_S|^2}, \quad (6)$$

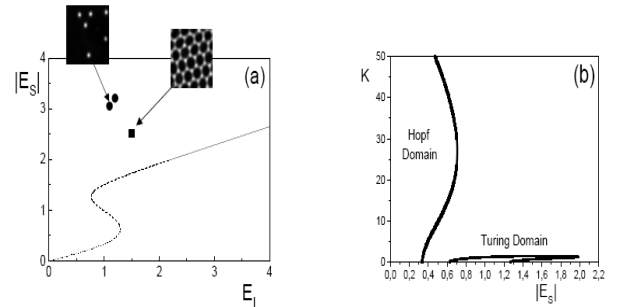


**Fig. 2** (a) Homogeneous stationary state: intracavity field amplitude  $|E_S|$  as a function of the injected holding beam amplitude  $E_I$ . The solid line portion of the S-curve is stable, the dashed line portion is unstable for Turing instability, the dotted line portion is unstable for Hopf instability. Symbols correspond to maximum intensity of patterns obtained by numerical simulations, displayed in the squares (honeycombs and CSs in this case). In (b) the Hopf and Turing domains affecting the stationary state are displayed in the plane  $(|E_S|, K)$ , where  $\vec{k}$  is the wave-vector of the perturbation. The values of  $|E_S|$  for which there exist values of  $K$  inside the domains are unstable. Parameters are:  $C = 0.45$ ,  $\theta = -2$ ,  $\alpha = 5$

$$j = 1.222, \quad d = 0.052, \quad \gamma_{\parallel}/\gamma_{\perp} = 0.0001, \quad \text{and} \quad \kappa/\gamma_{\perp} = 0.01$$

In order to determine the threshold value  $j_{th}$  and the laser frequency in absence of the injected field (free running regime) and in the plane-wave approximation we must set  $E_I = 0$  in the stationary equations of the model and consider the point where the nontrivial stationary solutions gives  $|E_S| = 0$ . We obtain:

$$j_{th} = \frac{1}{2C}, \quad (7)$$

$$\theta = -\alpha. \quad (8)$$

The calculation of  $|E_S|$  vs.  $E_I$  curve is obtained by

varying  $|E_s|$  as a free parameter. It turns out that, depending on the choice of the parameters, it can be S-shaped, as in the case displayed in Fig. 2 (a).

We then study the instabilities of the homogeneous steady state, which give rise either to another homogeneous state (plane-wave instability, PWI) or to a spatially modulated pattern (modulational instability, MI). To this aim, we perform the usual linear stability analysis of the system, by studying the response of the system to small spatially modulated fluctuations around the homogeneous solution

We obtain a fifth-order characteristic equation because we have five independent variables, that are the electric field and material polarization, their complex conjugates, and the carrier density. The characteristic equation reads:

$$\lambda^5 + a_4\lambda^4 + a_3\lambda^3 + a_2\lambda^2 + a_1\lambda + a_0 = 0, \quad (9)$$

where the coefficients  $a_i, i = 0, 1, 2, 3, 4$  depend on the system parameters  $\kappa, \gamma_{\parallel}, \gamma_{\perp}, \theta, \alpha, j, C, E_I, d, \Delta, \Gamma$  and on the modulus square  $K^2$  of the transverse wave-vector.

Let us fix all the values of the parameters with the exception of  $E_I$ ; instead of  $E_I$ , it is more convenient to consider the stationary value  $|E_s|$ , because  $E_I$  is a single-valued function of  $|E_s|$ , whereas  $|E_s|$  is, in general, a multi-valued function of  $E_I$ . In this way, the coefficients  $a_i (i = 0, 1, \dots, 4)$  are functions of the transverse wave-vector  $K$  and of  $|E_s|$ . We want to find the boundaries of the stability domains in the plane  $(|E_s|, K)$ .

The boundary of the Turing domain, corresponding to a stationary instability (real eigenvalue), is assigned by the condition  $\lambda = 0$  with  $\lambda$  real, which is in turn equivalent to  $a_0 = 0$ .

The boundary of the Hopf domain is assigned by the condition  $\lambda = i\nu$ . By substituting this expression in the characteristic Eq. (9) and after some simple algebra, we obtain the following stability boundary:

$$-(a_4a_1 - a_0)^2 + (a_4a_3 - a_2)(a_1a_2 - a_0a_3) = 0. \quad (10)$$

We explored different parametric regimes and found that the Hopf instability, typical of lasers above threshold, affects only the lower intensity branch of the homogeneous steady state, while the higher intensity branch is affected by a Turing instability, as it is shown in Fig. 2.

Parameters were chosen according to our previous studies on the same kind of micro-resonators, below threshold. As in [19] we set  $C = 45$ ,  $\mu = -2$ ,  $\alpha = 5$ , and  $d = 0.052$ . The injected current is considered around 10% above threshold, that in this case is  $j_{th} = 1.111$ . As for the decay rates, typical values for semiconductors are  $\gamma_{\perp}^{-1} = 100 \text{ fs}$  for the polarization decay time,  $\gamma_{\parallel}^{-1} = 1 \text{ ns}$  for carrier non-radiative recombination time and  $\kappa = 10 \text{ ps}$  for the cavity photon lifetime. We scale time in unit of  $\gamma_{\perp}^{-1}$  and the spatial variables by the diffraction length  $\sqrt{a}$ , with  $a = 20 \mu\text{m}$ .

The Hopf instability is characterized by a very high (but

finite) critical wave-number (see Fig. 2 (b)). It is worth noting that this critical wave-number has the same value as that destabilizing the trivial solution for the free-running laser case (no injection). In Fig. 3 we show the Hopf instability domain of the trivial homogeneous solution for  $E_I = 0$ , in the plane  $(j, K)$ , where  $j$  is the injected current. Two thresholds can be individuated: one is the plane-wave threshold  $j_{th} = 1.111$ , or the laser threshold in absence of diffraction, and it is given by the intersection with the  $x$ -axis. The other one, that is lower for this parameter choice ( $j_{th2} = 0.843$ ), is characterized by a critical wave-vector  $K_c$  different from zero ( $K_c = 26.6$ ), corresponding to an off-axis emission (traveling wave, TW) [20]-[21].

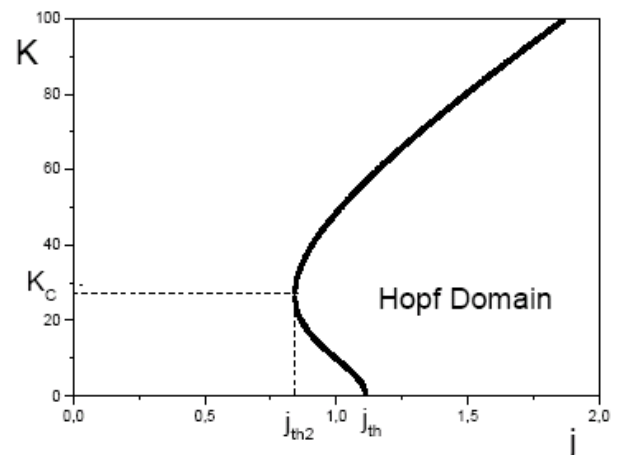


**Fig. 3** Hopf instability domain for the case of a free-running laser, plotted in the plane  $(j, K)$ , where  $j$  is the normalized injected current. In this case no field is injected, and the emitted frequency  $\omega_0$  is such that  $\theta = -\alpha$ . The other parameters are as in Fig. 2. Two different thresholds can be individuated: the plane-wave threshold  $j_{th} = 1.111$ , that is the laser threshold in absence of diffraction (it corresponds to  $K = 0$ ), and the TW threshold [20]  $j_{th2} = 0.843$ , that is lower for this parameter choice, corresponding to  $K_c = 26.6$ .

Coming back to the case with injected signal, we decided to reduce the injected current below the plane-wave threshold indicated by Eq. (7), and found that the Hopf domain survives (without any intersection with the  $x$ -axis, but keeping the same critical wave-vector  $K_c = 26.6$ ) until the other threshold  $j_{th2}$  is reached (see Fig. 4).

It is worth noting that this is a feature related to the consideration of the polarization dynamics: in the rate equation approximation no Hopf instability was found below the plane-wave threshold  $j_{th}$ . The rate equation approximation fails therefore to describe correctly the system dynamics, when diffraction is taken into account.

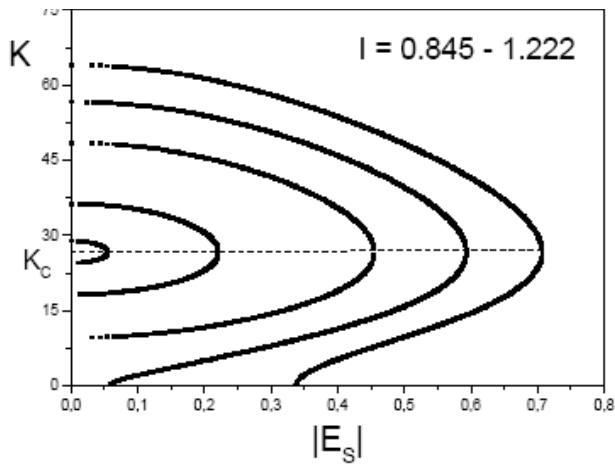


**Fig. 4** Hopf instability domains for different values of the injected current  $j$  ranging from  $j = 1.222$   $j$  (the largest domain) to  $j = 0.845$  (the smallest domain): the value of the critical wave-vector  $K_c = -26.6$  remains fixed. The Hopf domain vanishes for  $j \leq j_{th2} \approx 0.843$ . The other parameters are as in Fig. 2.

The critical wave-number characterizing the Hopf instability is strongly dependent on the ratio between the temporal parameters. In Fig. 5 we show the Hopf domain for three different values of the ratios  $\gamma_{\parallel}/\gamma_{\perp}$  and  $\kappa/\gamma_{\perp}$ . The instability threshold for  $|E_s|$  on the right remains fixed, but the value of the critical wave-vector  $K$  becomes smaller and smaller if the polarization dynamics is artificially slowed down. The homogeneous steady state and the Turing domain remain unchanged.

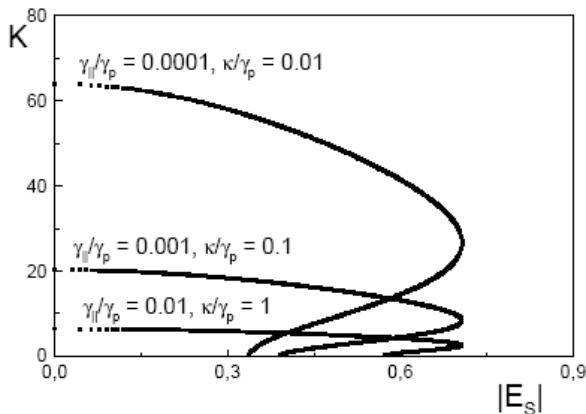


**Fig. 5** Hopf instability domains for different values of  $\gamma_{\parallel}/\gamma_{\perp}$  and  $\kappa/\gamma_{\perp}$ : the value of  $|E_s|$  for which the steady state becomes unstable remains fixed, but the critical wave-vector  $K_c$  becomes smaller and smaller if the polarization decay rate  $\gamma_{\perp}$  is decreased ( $\gamma_{\perp}$  is indicated as  $\gamma_p$  in the figure). The other parameters are as in Fig. 2.

#### IV. NUMERICAL RESULTS

We have performed the numerical integration of Eqs. (1)-(3) by using a split-step method with periodic boundary conditions. This method consists in separating the algebraic and the Laplacian terms in the right-hand side of Eqs. (1)-(3): the algebraic part is integrated using a Runge-Kutta algorithm, while for the Laplacian operator a 2-D FFT routine is adopted [25]. This implies that the

number of points for each side of the grid must be a power of 2, and we mostly assumed a  $64 \times 64$  grid.

The numerical integration of the complete problem is very demanding for the computational time required, because of the three very different time-scales involved, spanning over 4 orders of magnitude. Furthermore, for realistic values of the temporal parameters, the critical spatial wave-vector of the Hopf instability is very large ( $K_c \approx 26.6$ ), thus requiring a small space-step (that is, the distance between two neighboring points in the grid) to be able to resolve the spatial scale of the patterns.

Moreover, the algorithm converges only if the relation  $\delta t \leq \frac{\delta x^2}{4}$  holds, where  $\delta t$  is the time-step and  $\delta x$  is the space-step, used in the numerical simulations. In order to ensure proper stability and convergence of the algorithm, we chose a time-step  $\delta t \approx 10^{-2}$  and a space-step  $\delta x$  of 0.2–0.3.

Extended numerical results obtained by direct integration of the dynamical equations (1)-(3) show that stable CSs are possible in this regime, even if they sit on an unstable background (see Fig. 6). They can be obtained starting from a patterned initial condition (as the honeycombs in Fig. 2 (a)), by reducing the input field amplitude.

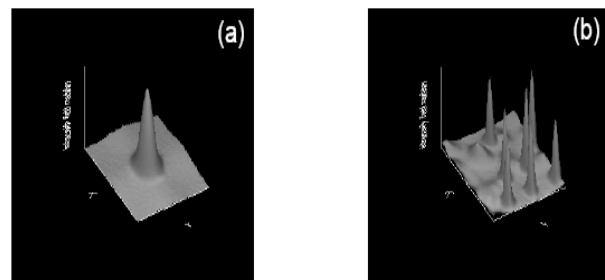


**Fig. 6** Intracavity field amplitude profile in the case of one (a) or several (b) CSs: they sit on unstable background. Parameters are as in Fig. 2.

The soliton peak intensity turns out to be almost constant, while the background is rapidly oscillating (see Fig. 7).

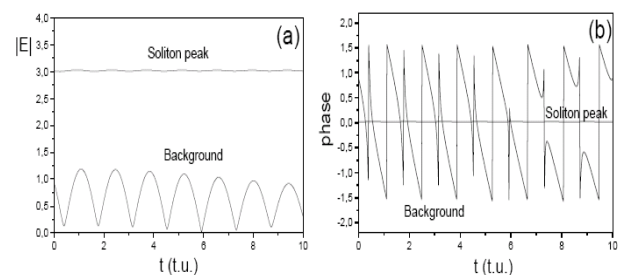


**Fig. 7** Temporal behavior of field amplitude (a) and phase (b) of the background and CS peak.

Despite the instability affecting the background, it turns out to be perfectly possible to write and erase CSs in the usual manner. A writing beam (WB) is injected into the cavity, with the same phase as the holding field, for a certain time (ranging from half to several nanoseconds),

then it is removed. The CS grows up and remains fixed at the location where the WB was injected. There is a good tolerance with respect to the WB phase: it is possible to excite CSs with phase ranging from 0 to almost  $\pi/2$ . To erase CSs, we proceed in the usual way: the WB is injected again at the CS position, but with an opposite phase with respect to the holding beam. The CS disappears and it remains off also when the erasing beam is removed.

## V. CONCLUSION

We studied here the transverse dynamics of a driven broad-area VCSEL above threshold, where dynamical instabilities take place and the rate-equation approximation fails to correctly describe the system dynamics in presence of diffraction. We therefore considered also the material polarization dynamics, by using a model introduced by Agrawal, characterized by 5 dynamical equations, similar to a simple two level model but containing all the information concerning the physics of semiconductors.

We studied the homogeneous stationary state and their instabilities, both stationary (Turing) and dynamical (Hopf). We found some parametric regimes where the homogeneous steady state is bistable, with the lower branch unstable for a Hopf instability, and the upper branch unstable for Turing instability.

When the dynamical equations are integrated numerically, patterns can be obtained for higher input field intensities, where the steady state is affected by a Turing instability. Cavity solitons are also possible, but they are sitting on a background that is dynamically unstable. CSs intensity and phase are basically constant, while the background is rapidly oscillating.

Despite the instability affecting the background, CSs can be written and erased in the usual way, by means of writing and erasing beams.

Therefore CSs result to be robust structure and possible candidates for optical information treatment also in VCSELS above threshold, where a larger power of emission is available.

## ACKNOWLEDGMENTS

This work was carried out in the framework of the ESPRIT LTR Project n.28235 PIANOS, the PRIN project *Formazione e controllo di solitoni di cavit`a in microrisonatori a semiconduttore* of the Italian Ministry for University and Research, and the European Network VISTA (VCSELS for Information Society Technology Applications).

Reza Kheradmand undertook this work with the support of the "ICTP Programme for Training and Research in Italian Laboratories, Trieste, Italy".

## VI. REFERENCES

- [1] F. Arecchi, "Space-time complexity in nonlinear optics," *Physica D* 51, pp. 450–464, 1991.
- [2] L. A. Lugiato, "Spatio-temporal structures: I.," *Phys. Rep.* 219, pp. 293–310, 1992.
- [3] L. A. Lugiato, M. Brambilla, and A. Gatti, "Optical pattern formation," 40, pp. 229–306, Academic Press, New York, 1998.
- [4] J. Moloney and H.M.Gibbs, "Role of diffractive coupling and self-focusing or defocusing in the dynamical switching of a bistable optical cavity," *Phys. Rev. Lett.* 48, pp. 1607–1610, 1982.
- [5] D. M. Laughlin, J. Moloney, and A. Newell, "Solitary waves as fixed points of infinite-dimensional maps in an optical bistable ring cavity," *Phys. Rev. Lett.* 51, pp. 75–78, 1983.
- [6] N. Rosanov and G. Khodova, "Auto solitons in bistable interferometers," *Opt. Spectroscop.* 65, pp. 449–450, 1988.
- [7] M. Tlidi, P. Mandel, and R. Lefever, "Localized structures and localized patterns in optical bistability," *Phys. Rev. Lett.* 73, pp. 640–643, 1994.
- [8] W. Firth and A. Scroggie, "Optical bullet holes: robust controllable localized states of a nonlinear cavity," *Phys. Rev. Lett.* 76, pp. 1623–1626, 1996.
- [9] V. Taranenko, K. Staliunas, and C. Weiss, "Spatial soliton laser: localized structures in a laser with a saturable absorber in a self-imaging resonator," *Phys. Rev. A* 56, pp. 1582–1591, 1997.
- [10] K. Staliunas and V. Sanchez-Morcillo, "Localized structures in degenerate optical parametric oscillators," *Opt. Commun.* 139, pp. 306–312, 1997.
- [11] C. Etrich, V. Peschel, and F. Lederer, "Solitary waves in quadratically nonlinear resonators," *Phys. Rev. Lett.* 79, pp. 2454–2457, 1997.
- [12] M. Brambilla, L. Lugiato, F. Prati, L. Spinelli, and W. Firth, "Spatial soliton pixels in semiconductor devices," *Phys. Rev. Lett.* 79, pp. 2042–2045, 1997.
- [13] M. Saffman, D. Montgomery, and D. Anderson, "Collapse of a transverse-mode continuum in a self-imaging photorefractively pumped ring resonator," *Opt. Lett.* 19, pp. 518–520, 1994.
- [14] C. Weiss, M. Vaupel, K. Staliunas, G. Sleky, and V. Taranenko, "Solitons and vortices in lasers," *Appl. Phys. B* 68, pp. 151–168, 1999.
- [15] J. Grantham, H. Gibbs, G. Khitrova, J. Valley, and X. Jiajin, "Kaleidoscopic spatial instability: bifurcations of optical transverse solitary waves," *Phys. Rev. Lett.* 66, pp. 1422–1425, 1991.
- [16] Schreiber, B. Thuring, M. Kreuzer, and T. Tschudi, "Experimental investigation of solitary structures in a nonlinear optical feedback system," *Opt. Commun.* 136, pp. 415–418, 1997.



- [17] Schaeppers, M. Feldman, T. Ackemann, and W. Lange, "Interaction of localized structures in an optical pattern-forming system," *Phys. Rev. Lett.* 85, pp. 748–751, 2000.
- [18] S. Barland, J. Tredicce, M. Brambilla, L. Lugiato, S. Balle, M. Giudici, T. Maggipinto, L. Spinelli, G. Tissoni, T. Knoedl, M. Miller, and R. Jaeger, "Cavity solitons as pixels in semiconductor microcavities," *Nature* 419, pp. 699–702, 2002.
- [19] L. Spinelli, G. Tissoni, M. Brambilla, F. Prati, and L. Lugiato, "Spatial solitons in semiconductor microcavities," *Phys. Rev. A* 58, pp. 2542–2559, 1998.
- [20] P. Jakobsen, J. Lega, Q. Feng, J. Moloney, and A. Newell, "Nonlinear transverse modes of large-aspect-ratio homogeneously broadened lasers: I. analysis and numerical simulation," *Phys. Rev. A* 49, pp. 4189–4200, 1994.
- [21] J. Lega, P. Jakobsen, J. Moloney, and A. Newell, "Nonlinear transverse modes of large-

aspect-ratio homogeneously broadened lasers: II. pattern analysis near and beyond threshold," *Phys. Rev. A* 49, pp. 4201–4212, 1994.

- [22] G. D'Alessandro, A. Kent, and G.-L. Oppo, "Centre manifold reduction of laser equations with transverse effects: an approach based on modal expansion," *Opt. Commun.* 131, pp. 172–194, 1996.
- [23] G. van Tartwijk and G. Agrawal, "Laser instabilities: a modern perspective," *Progress in Quantum Electronics* 22, pp. 43–122, 1998.
- [24] J. Yao, G. A. P. Gallion, and C. Bowden, "Semiconductor laser dynamics beyond the rate-equation approximation," *Optics Commun.* 119, pp. 246–255, 1995.
- [25] W. Press, B. Flannery, S. Teukolsky, and W. Vetterling, *Numerical Recipes*, Cambridge University Press, Cambridge, 1986.

Currently, he is a Researcher with the the University of Tabriz, Iran. His activity concerns the theory of cavity solitons in semiconductor microresonators.



**Giovanna Tissoni** received the Laurea and the Ph.D. degrees from the University of Milan, Milan, Italy, in 1995 and 1998, respectively, both in physics. She is currently a Researcher at the INFN Research Unit, University of Insubria, Como, Italy. Since 1997, she has been dealing with semiconductor modeling and applications to transverse pattern and cavity

soliton formation in semiconductor microresonators. She has coauthored about 30 publications in international journals and proceedings and has participated in several international conferences and national and European projects. Her research activities began with the study of transverse and polarization properties of the light emitted by vertical-cavity semiconductor lasers (VCSELs). She has been a member of the National Institute of Physics of Matter (INFN, now CNR) since 1995.



**Massimo Brambilla** received the Laurea degree in physics from the University of Milan, Milan, Italy, in 1988, and the Ph.D. degree in physics from the University of Zurich, Zurich, Switzerland, in 1992.

He is currently an Associate Professor with the Engineering Faculty of the Polytechnic of Bari, Bari, Italy. He has coordinated or participated in several

national and European projects with the groups of Milan (1988–1995) and Bari (1995–present). In particular, he has been active in ESPRIT and FET projects. He has coauthored about 90 publications in international journals and proceedings. His research activities cover dynamical instabilities in optical bistability and lasers, pattern formation in nonlinear optical systems; during the last eight years, his research has focused on the study of localized structures formation in semiconductor-based microresonators and the application thereof to all-optical information treatment.



**Igor Protsenko** received the Ph.D. degree in physics from the Lebedev Physical Institute of RAS, Moscow, Russia, in 1989.

He is currently a Senior Researcher in the Lebedev Physical Institute, Joint Institute of Nuclear Research, Dubna, Russia, and a Lecturer of Theoretical Quantum Electronics course at the Moscow Engineering and Physics Institute. He is a

co-author of about 50 publications in international refereed journals. He is the holder of ten patents. His research interests are in the theory of quantum radiation-matter interaction, laser nonlinear dynamics, and new optical materials (nanoplasmonics).



**Luigi A. Lugiato** received the Laurea degree in physics from the University of Milan, Milan, Italy, in 1968.

He is currently a Professor of Quantum Electronics at the University of Insubria, Como, Italy, and the Director of the National Institute of Physics of Matter (INFN) Research Unit, Como, Italy. He is the author of more than 350 publications in international refereed journals and

conference proceedings. His research activities are mainly in the fields of nonlinear and quantum optics, contributing to the topics of superfluorescence, optical bistability, squeezing, optical instabilities, optical pattern formation, cavity solitons, and quantum imaging.



**Reza Kheradmand** received the Ph.D. degree in physics from the University of Tabriz, Tabriz, Iran, in 2005.

From November 2002 to November 2003 and from February 2005 to July 2005, he was an ICTP (Abdus Salam International Center for Theoretical Physics, Trieste, Italy) Research Fellow at the University of Insubria, Como, Italy. He was also associated with the INFN-National Institute for the Physics of Matter, Italy.